

# The RISING Project

A double-sided Si-strip detector as an active stopper



R. Kumar<sup>1,2</sup>, F.G. Molina<sup>3</sup>, S. Pietri<sup>4</sup>, P. Dooenbal<sup>2,5</sup>,

I. Kojucharov<sup>2</sup>, W. Prokopowicz<sup>2</sup>, H. Schaffner<sup>2</sup> and

H.-J. Wollersheim<sup>2</sup>

<sup>1</sup>IUAC New Delhi, <sup>2</sup>GSID armstadt, <sup>3</sup>Univ. Valencia, <sup>4</sup>Univ. Surrey,

<sup>5</sup>Univ. Köln

September 2006

## 1. Introduction

A new beta counting system has been developed for the RISING (Rare Isotope Spectroscopic Investigation at GSI) project to study the beta decay of exotic nuclei produced by fission and fragmentation. This system employs the Micron Semiconductor Ltd. [1] Model W1(DS)-1000 DC coupled double-sided silicon strip detector (DSSSD) with 16 front strips and 16 back strips, each of width 3mm (see fig. 2), to detect both fragmentation plants and their subsequent beta decays. One of the challenges in designing electronics for the beta counting system is the range of charged particle energies that must be measured. A fast fragmentation plant will deposit more than 1 GeV total energy in the DSSSD, while an emitted beta particle will deposit less than 1 MeV. As can be seen in fig. 1, implantation and decay events are directly correlated within each pixel of the detector, providing a measurement of the  $\beta$ -decay time in the seconds range. Measurements with mesytc [2] and Multi Channel Systems [3] electronics will be described and experimental results of a  $^{241}\text{Am}$   $\alpha$ -source and  $^{207}\text{Bi}$   $\beta$ -source are discussed. Finally, a measurement with  $^{136}\text{Xe}$  ions was performed which were implanted in the DSSSD.

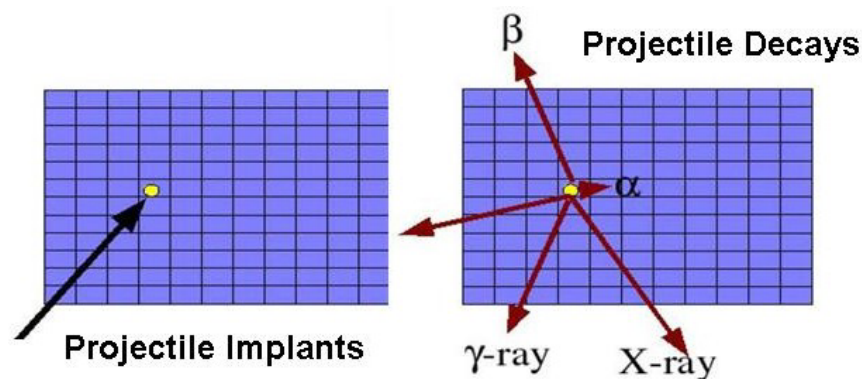


**Fig 1:** Schematic drawing of the position correlation between the projectile implant and the subsequent  $\beta$ -decay measured with the double-sided silicon strip detector (DSSSD).

## 2. Double-sided Si-strip detector W1(DS)-1000

The DSSSD W1(DS)-1000 provides 256  $3 \times 3 \text{ mm}^2$  pixels on the  $5 \times 5 \text{ cm}^2$  detector to encode x-y position (see fig. 2). A thickness of 1000  $\mu\text{m}$  is used to ensure sufficient silicon for detection of the high-energy  $\beta$ -particles (MeV range) expected from the decay of radioactive nuclei. The detector was run at a bias voltage of 200V to obtain full depletion.



**Fig 2:** Schematic drawing of the W1(DS)-1000 double-sided silicon strip detector (DSSSD) from Micron Semiconductor Ltd. [1].

The DSSSD was mounted to a special detector adapter designed by mesytec [2]. The strips were connected by two 20 pole flat ribbon connectors to the pre-amplifiers. The used mesytec cabling collection consists of three main components:

- Shielded multipole cables for in- and outside the vacuum vessel
- Several types of selected vacuum feedthroughs
- Individually designed detector adapters

### 3. Measurements with mesytec electronics

The mesytec MPR-32 preamplifier was used for the 16 front and 16 back strips of a single DSSSD. Positive and negative charge can be amplified equally. The input connectors are subD 25 female connectors. For the differential outputs twisted pair 34 pin male header connectors are used. For a  $^{207}\text{Bi}\beta$ -source the MPR-32 output signal is displayed in fig. 3 with a pulse height of approximately 200mV and a decay time of 30 $\mu\text{s}$ . The signal to noise ratio is 10:1.

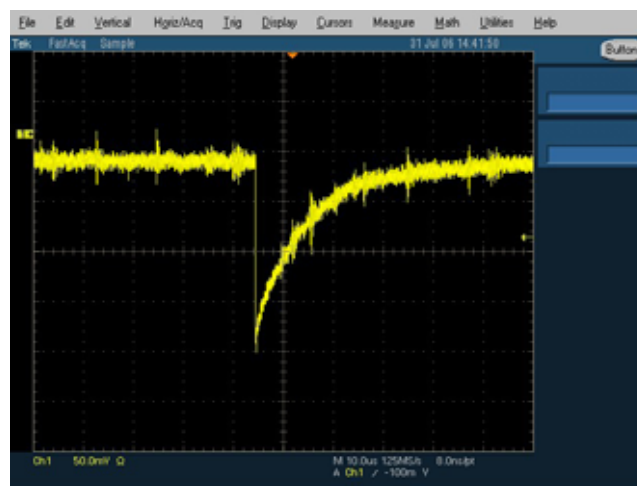


**Fig 3:** Output signal of the MPR-32 preamplifier for a  $^{207}\text{Bi}\beta$ -source (pulse-height 200mV, decay time 30 $\mu\text{s}$ ).

The mesytec MPR-32 multi-channel preamplifier is available in a linear and logarithmic mode. A typical application of the logarithmic one is decay spectroscopy which allows the measurement of both the  $\beta$ -energy (in MeV range) and the implantation of heavy ions (in GeV range) with the silicon detector. The MPR-LOG series provides a linear range, which covers 70% of the total range. The last 30% covers the range up to 3 GeV. Fig 4 shows the characteristics of the logarithmic MPR-32 preamplifier which was measured with a research pulser using the correct pulse shape. The pulse height can not be directly related to the implantation energy because of the pulse height defect. Appendix E shows the maximum incident energy for heavy ions implanted in 0.5mm and 1mm silicon. A switch at the logarithmic MPR-32 preamplifier allows choosing a linear range of 2.5 MeV or 10 MeV. For the linear MPR-32 preamplifier an amplification range of 5 MeV and 25 MeV can be chosen.

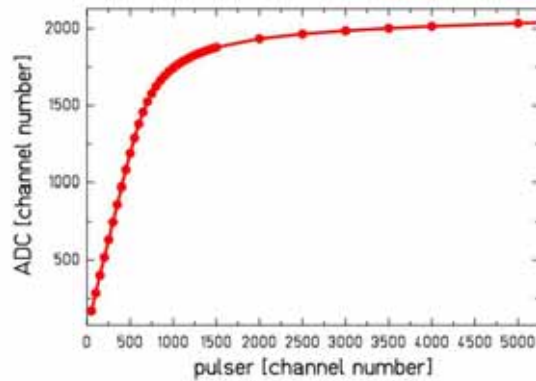


**Fig 4** The characteristics of the logarithmic MPR-32 preamplifier was measured with a 10MeV linear range setting and the STM-16 spectroscopy amplifier (gain= 1, threshold= 5 and shaping time 2.5 $\mu$ s FWHM).

The MPR-32 can easily be combined with two mesytec STM-16 shaping-/timing filter/discriminator modules when the differential input version is used. The input resistance must be terminated with 50 $\Omega$  for the linear MPR-32 and 100 $\Omega$  for the logarithmic MPR-32. The polarity can be changed with a 4\*16 pole connector (inside the case labelled differential input gain 2). Two shaping times of  $\sigma=0.4\mu$ s/ $1\mu$ s (1.0 $\mu$ s/2.5 $\mu$ s FWHM) can be selected by a jumper (short/long) which is common for all channels. For the following measurements a shaping time of 1 $\mu$ s (FWHM) was selected.

The STM-16 can be controlled by a NIM-module MRC-1 which works as a bus master. One mesytec MRC-1 can control 32 various mesytec modules (not only STM-16). It is prepared for the remote control of (i) individual discriminator thresholds (0% to 40% of maximum range, 4V) and (ii) gains (in 16 steps) for pairs of channels. Communication with a control PC is done via RS-232 serial interface.

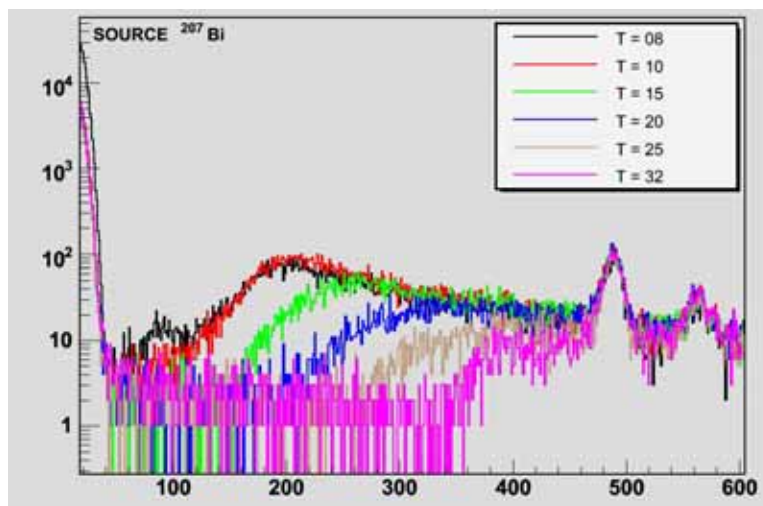


**Fig 5:** Energy spectrum of a  $^{207}\text{Bi}$   $\beta$ -source measured for different discriminator thresholds labelled T= 8 to T= 32 of the mesytec STM-16 module.

Each analogue signal (34 pin male connector) was fed directly to a CAEN V785A ADC. The trigger signal of STM-16 was used to produce the ADC gate. Details of the electronic modules and the electronics diagram can be found in Appendix A and B. Fig 5 shows the

energy spectrum of a  $^{207}\text{Bi}$   $\beta$ -source measured for different discriminator thresholds of the mesytec STM -16 module. The detection limit seems to be at around 150keV .

### 3.1 Results with mesytec electronics

#### 3.1.1 Energy resolution measured with $\alpha$ -particles of a $^{241}\text{Am}$ source

The energy resolution of the individual strips was measured by a thin  $^{241}\text{Am}$  source placed 5cm from the detector's surface in a vacuum vessel, flooding it with  $\alpha$ -particles. The range of 5MeV  $\alpha$ -particles in silicon is  $\approx 28\mu\text{m}$  . A Gaussian function was fit to the 5.486MeV peak . Individual strips displayed energy resolutions of 0.48-0.52% (front) and 0.51-0.64% (back) FWHM for the 5.486MeV peak . The edge strips showed a somewhat poorer resolution . Typical  $\alpha$ -energy spectra for individual strips are displayed in fig.6 . Neighbouring strips are separated by an insulating gap . It has already been observed by others [4] that a charged particle entering the detector through the gap between the strips induces a reduced pulse height in the front strips in comparison to a particle entering through a strip . This effect is believed to be the result of charge trapping between strips due to the shape of the electric field between the strips . We have also observed this effect (see fig.6 left) .

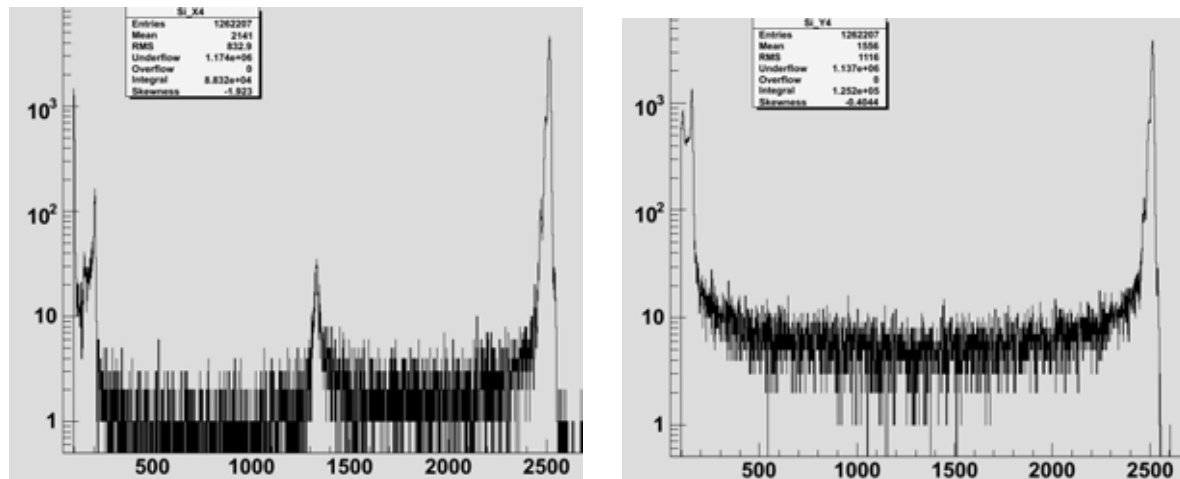


Fig.6: Energy spectrum of a  $^{241}\text{Am}$   $\alpha$ -source measured with DSSSD -2512-17 front strip X4 (left) and back strip Y4 (right) .

For a fully depleted DSSSD (bias voltage 200V) the strip multiplicity is close to unity, while the maximum of the strip multiplicity (back side) is shifted to 2 for a detector bias voltage of 40V (fig.7) .

The relative efficiency of the strips is roughly constant across the entire detector as it was examined by C. Wrede et al. [4] . Therefore, the distribution of the  $\alpha$ -source can be examined with a resolution of 256 pixels . Data were taken under the following condition : First, the  $^{241}\text{Am}$  source was centred relative to the DSSSD and second, moved to one side of the DSSSD . Fig.8 shows both 3-D histograms of x-position versus y-position . One can clearly see the intensity distribution and the boundaries of the  $\alpha$ -source .

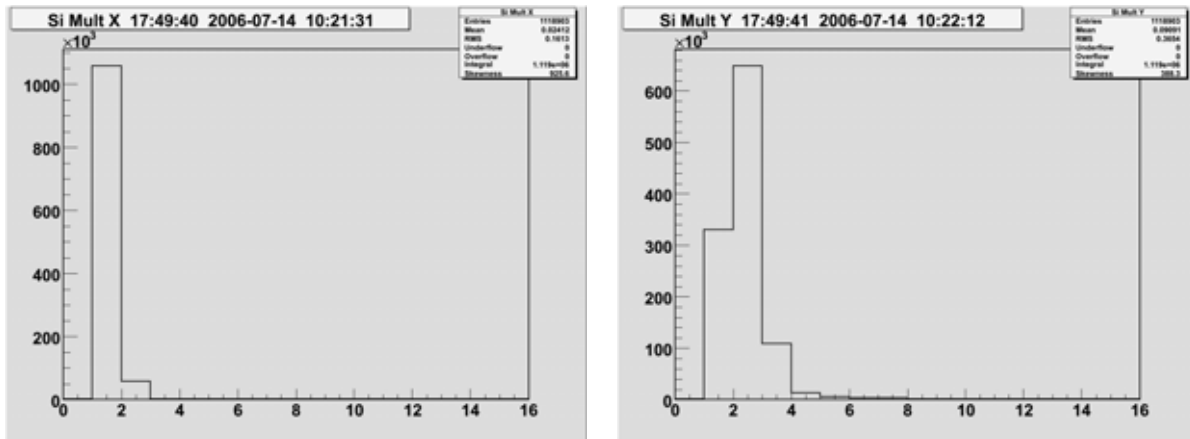


Fig.7: Strip multiplicity for front (left) and back (right) side measured for D SSSD -2512-17 at a bias voltage of 40V (detector not fully depleted) for  $\alpha$ -particles of a  $^{241}\text{Am}$  source.

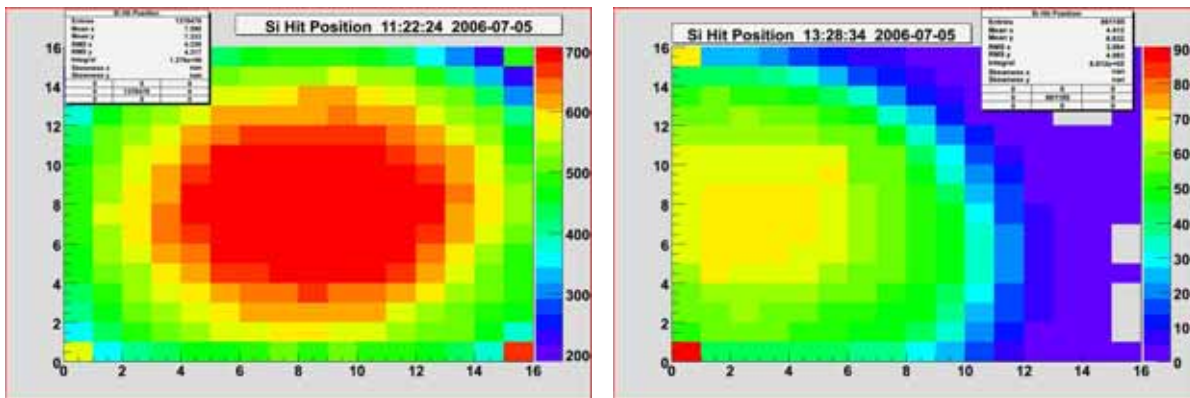
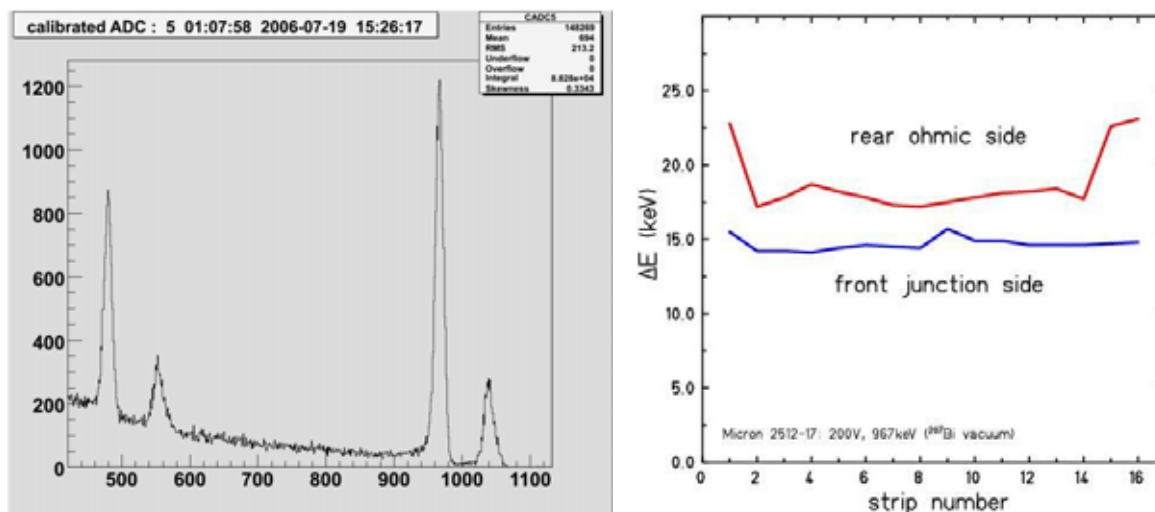


Fig.8: 3-D histogram of x-position versus y-position measured for D SSSD -2243-5 with  $\alpha$ -particles of a  $^{241}\text{Am}$  source. The source is centred (left) and off-centre (right) relative to the D SSSD .

### 3.1.2 Energy resolution measured with electrons of a $^{207}\text{Bi}$ source

A  $^{207}\text{Bi}$  conversion electron source (Appendix I) which emits mono-energetic  $\beta$ -particles was used to calibrate the D SSSD . The  $^{207}\text{Bi}$  source was positioned about 5cm from the front face of the detector. The measured electron spectrum for strip X 4 is shown in fig.9. Four peaks (482keV , 555keV , 976keV and 1049keV ) are clearly seen and are due to K and L conversion electrons of the 570keV and 1060keV transition in  $^{207}\text{Pb}$ . For the maximum beta energy of 1049keV a detector thickness of  $\approx 2.31\text{mm}$  is required. Since the path of a beta particle is not a straight line, it is not absolutely essential that the detector has the indicated thickness. The energy resolution of the 976keV line is 14.4keV for strip X 4. Fig.9 shows an overview of the energy resolution versus the strip number which is better for the front junction side than the rear ohmic side.





**Fig 9:** The conversion electron spectrum of  $^{207}\text{Bi}$  obtained by strip X4 of D SSSD -2512-17. Four peaks at 482keV , 555keV , 976keV and 1049keV are by mono-energetic electrons (left). The energy resolution for the front junction and the rear ohmic side versus the strip number is plotted on the right side.

If the measurements were performed with a detector (D SSSD -2243-5) which was already exposed to a heavy ion beam , the average energy resolution is 16.2keV for the front junction side and 33.3keV for the rear ohmic side (fig.10).

All data discussed so far were obtained for a detector in vacuum .D SSSD -2243-5 was also investigated in dry nitrogen and the results are also displayed in fig.10 .The energy resolution measured in vacuum and dry nitrogen is the same within the experimental uncertainties.

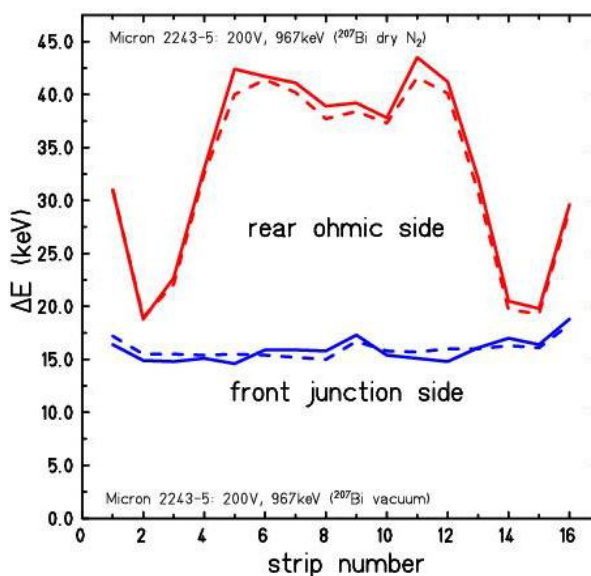


**Fig 10:** The energy resolution of D SSSD -2243-5 for the front junction and the rear ohmic side is plotted versus the strip number. The measurements were performed in vacuum (full line) and in dry nitrogen  $\text{N}_2$  (dashed line)

In conclusion , the proposed RISING experiments with an active stopper should be performed in dry nitrogen , which allows the use of a detector vessel with thin walls to minimize the absorption of the emitted  $\gamma$ -rays.

The comparison between the linear and logarithmic MPR-32 preamplifier is displayed in fig.11, which shows a slightly worse energy resolution for the logarithmic one, 19.7keV instead of 15.3keV. However, the logarithmic MPR-32 has the advantage to measure both the implantation energy as well as the  $\beta$ -energy.

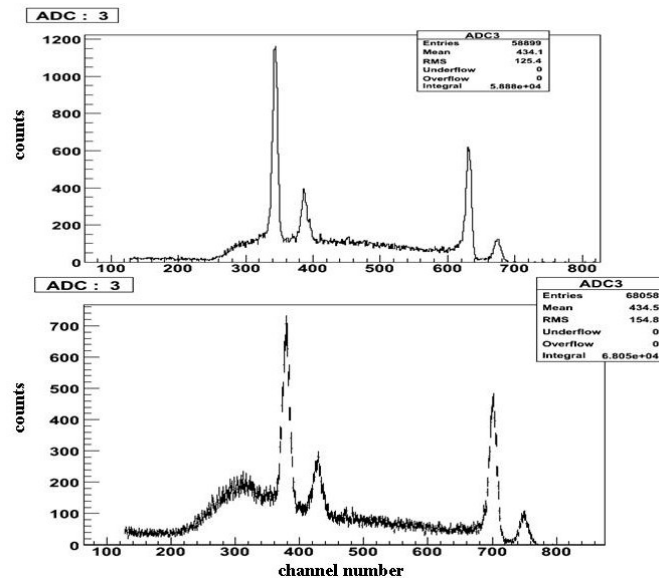


**Fig 11:** The conversion electron spectrum of  $^{207}\text{Bi}$  obtained by strip X3 of DSSSD -2243-5 m measured with the linear MPR-32 (top) and the logarithmic MPR-32 (bottom). The energy resolution and the signal-to-noise ratio are  $\Delta E = 15.3\text{keV}$  and 3.5:1 for the linear MPR-32 and  $\Delta E = 19.7\text{keV}$  and 2.6:1 for the logarithmic MPR-32, respectively.

#### 4. Measurements with MultiChannel Systems electronics

At the National Superconducting Cyclotron Laboratory (NSCL) at Michigan State University (MSU) a new counting system [5] has been developed which yields reliable energy information for both implants and decays. The DSSSD signals are first processed by two 16-channel charge sensitive preamplifier modules CPA-16 supplied by MultiChannel Systems. These modules contain precision pre- and shaping amplifier electronics and provide both high gain (2V/pC) and low gain (0.1V/pC) analogue outputs. One module was specified to have inverted output signals, and the other one non-inverted, so that the processed outputs from both the front and backsides of the DSSSD share the same polarity. For a  $^{207}\text{Bi}$   $\beta$ -source the CPA-16 output signal is displayed in fig.12 with a pulse height of approximately 200 mV and a width of about 1  $\mu\text{s}$ . Therefore, a high counting rate of at least 100 kHz can be applied without pulse pile-up. The signal to noise ratio is 7:1. As a result, the low gain signals, which provide the fast fragment implantation energy information, can be sent directly to CAEN V785A ADC with no further shaping. As the high gain signals carry information from low-energy beta decay events, they require further processing. This is accomplished at MSU using Pico Systems [6] 16-channel shaper/discriminator modules in CAMAC. The shaper output of the Pico System module is sent directly to an ADC while each discriminator output is combined in a logical OR gate to provide the master trigger. Since Pico System modules were not available at GSI, ORTEC 572 and 16-channel CAEN N568BC amplifiers were used for further shaping the high gain CPA-16 output signals. Details of the electronic modules and the electronics diagram can be found in Appendix C and D.



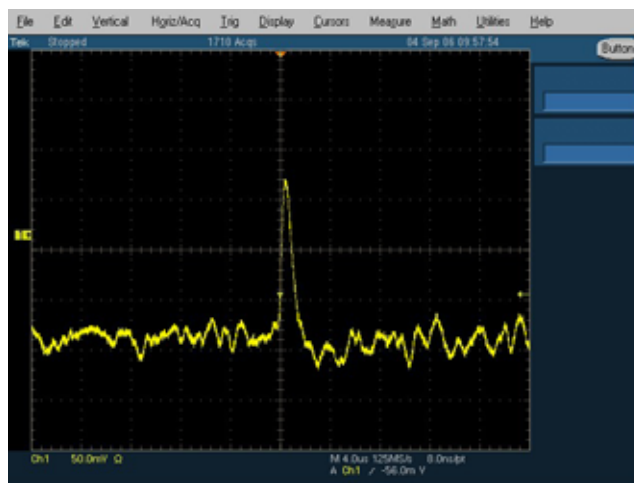


Fig 12: Output signal of the CPA -16 preamplifier for a  $^{207}\text{Bi}$   $\beta$ -source.

## 4.1 Results with MultiChannelSystem electronics

### 4.1.1 Energy resolution measured with $\beta$ -particles of a $^{207}\text{Bi}$ source

A  $^{207}\text{Bi}$  conversion electron source was used to measure the electron spectrum for one representative strip of DSSSD -2243-5 (fig 13). The  $\beta$ -source was also positioned about 5cm from the front face of the detector. Three different measurements were performed: (i) the high gain output signal of the CPA -16 preamplifier was sent directly to the ADC, (ii) it was additionally amplified with ORTEC 572 using shaping times of 0.5 $\mu\text{s}$ , 1.0 $\mu\text{s}$  and 2.0 $\mu\text{s}$ , respectively and (iii) with CAEN N 568BC with shaping time 2.0 $\mu\text{s}$  before sending it to the ADC. Fig 13 shows the conversion electron spectrum of  $^{207}\text{Bi}$  without further amplification. Only two peaks (482keV and 976keV) are clearly seen and are due to K conversion electrons of the 570keV and 1060keV transition in  $^{207}\text{Pb}$ . The energy resolution of the 976keV line is 100keV. The detection limit seems to be at around 300keV.

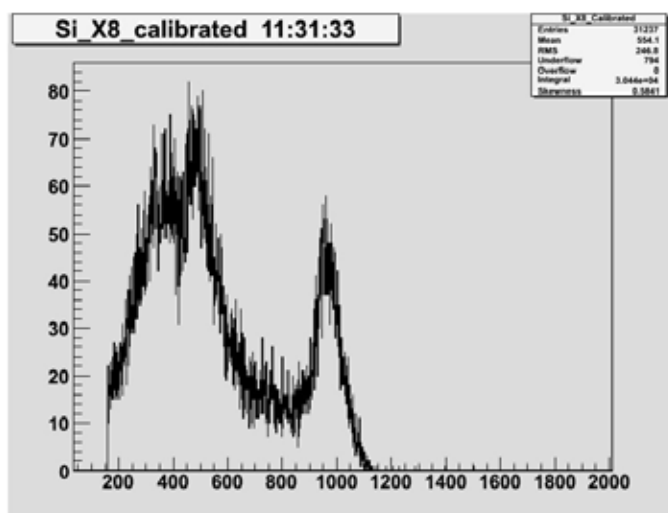


Fig 13: The conversion electron spectrum of  $^{207}\text{Bi}$  obtained by a strip of DSSSD -2243-5. Two peaks at 482keV and 976keV are by mono-energetic electrons. The high gain output signal of the CPA -16 preamplifier was sent directly to the ADC.

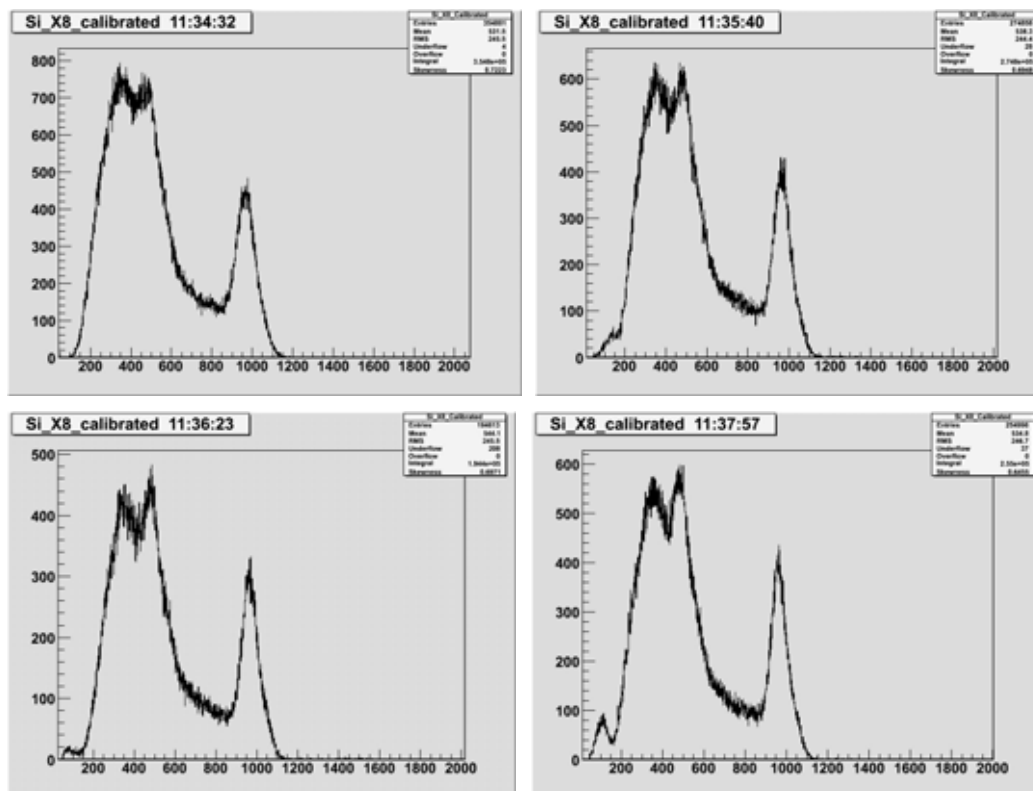


Fig 14 : Conversion electron spectra of  $^{207}\text{Bi}$  obtained by a strip of DSSSD -2243-5. The high gain output signal of the CPA -16 preamplifier was amplified with ORTEC 572 using shaping times of  $0.5\mu\text{s}$  (top left),  $1.0\mu\text{s}$  (top right) and  $2.0\mu\text{s}$  (bottom left) and with CAEN N568BC with shaping time  $2.0\mu\text{s}$  (bottom right) before sending to the ADC .

Fig. 14 shows conversion electron spectra after additional amplification with ORTEC 572 and CAEN N568BC . The measured energy resolutions are summarized in the table below .

shaping time [ $\mu\text{s}$ ]	ORTEC 572	CAEN N568BC
0.5	122 keV	
1.0	112 keV	
2.0	103 keV	113 keV

In conclusion, for the DSSSD an energy resolution of 15keV and an energy threshold of 150keV have been measured for the mesytec electronic which compares to a FWHM of 100keV and a threshold of 300keV for MultiChannelSystem electronics.

## 5. Chamber for the RISING active stopper

After the decision to operate the DSSSD in dry nitrogen,  $\gamma$ -transmission measurements were performed with  $^{57}\text{Co}$  ( $E_\gamma=0.122, 0.136\text{ MeV}$ ) and  $^{60}\text{Co}$  ( $E_\gamma=1.173, 1.332\text{ MeV}$ ) sources. Different aluminium plates varying between 1mm and 5mm as well as printed circuit board material Pertinax (phenolic-formaldehyde-cellulose-paper PFCP 2061) of 6mm thickness were irradiated and the non-absorbed  $\gamma$ -rays were detected in a Geiger-Müller counter. The ratio of the  $\gamma$ -transmission of aluminium and Pertinax is plotted in fig.15 as a function of the Al-layer thickness. The  $\gamma$ -transmission of both materials is equal for a thickness of 2mm aluminium .

Since the chamber of the active stopper can be produced with Pertinax of 2mm thickness, the aluminium equivalent is 0.7mm. Fig.16 shows the active stopper chamber produced out of 2mm Pertinax with an entrance and exit window covered by a thin black Pocalon C foil (20µm). The top cover of the chamber shows the cable connectors for six DSSD which can be arranged in two rows.

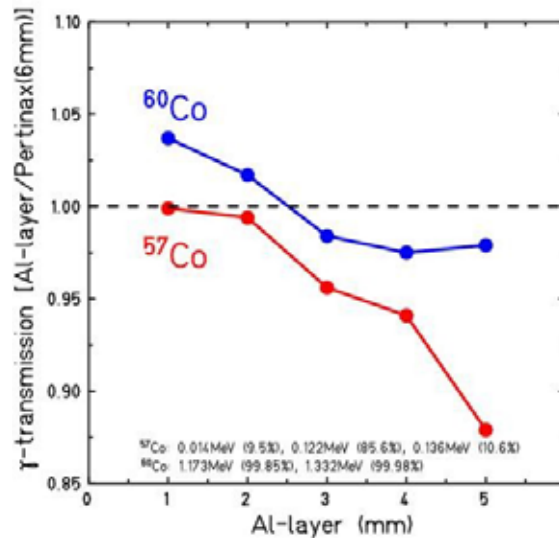


Fig.15: The ratio of the  $\gamma$ -transmission of aluminium and the printed circuit board material Pertinax is plotted as a function of the Al-layer. The  $\gamma$ -transmission of both materials is equal for a thickness of 2mm aluminium.

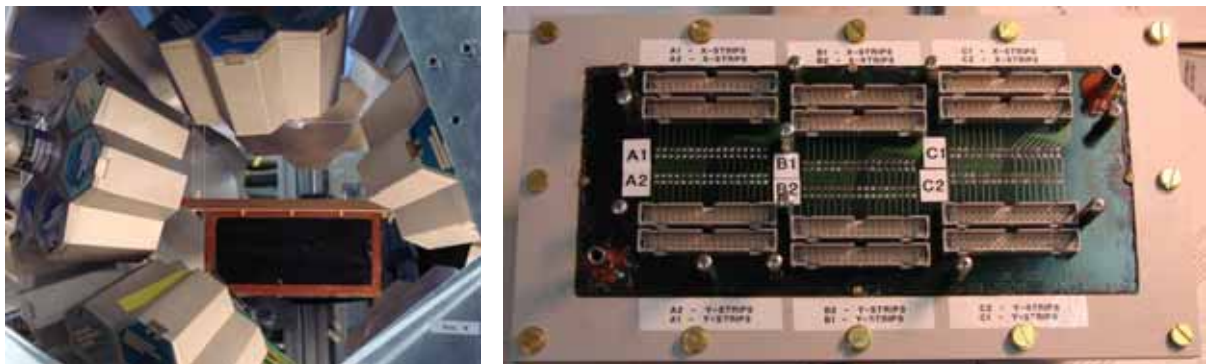


Fig.16: The Cluster array of the stopped beam RISING experiments with the active stopper vessel made out of Pertinax (left) and the top cover of the active stopper chamber with the cable connectors (right) for six DSSD arranged in two rows.

A  $^{207}\text{Bi}$  conversion electron source was mounted in front of the new Pertinax chamber and the electron spectrum was measured for DSSD-2243-2. The mesytec electronic was used to obtain the energy resolution which yields an average value of 15.1keV for the front junction side (X-strips).

## 6. Implantation measurement with a $^{136}\text{Xe}$ beam

A test measurement has been performed with the RISING set-up (fig.17) in the S4 area of the fragment separator (FRS) at GSI to investigate the heavy ion implantation in the double-sided Si-strip detector. A primary beam of  $^{136}\text{Xe}$  with 400AMeV was used to be slowed down in the

S4-degrader and finally implanted in the silicon detector. The active stopper vessel for the DSSSD is shown in fig.16 surrounded by the Cluster array of the stopped beam RISING experiments.

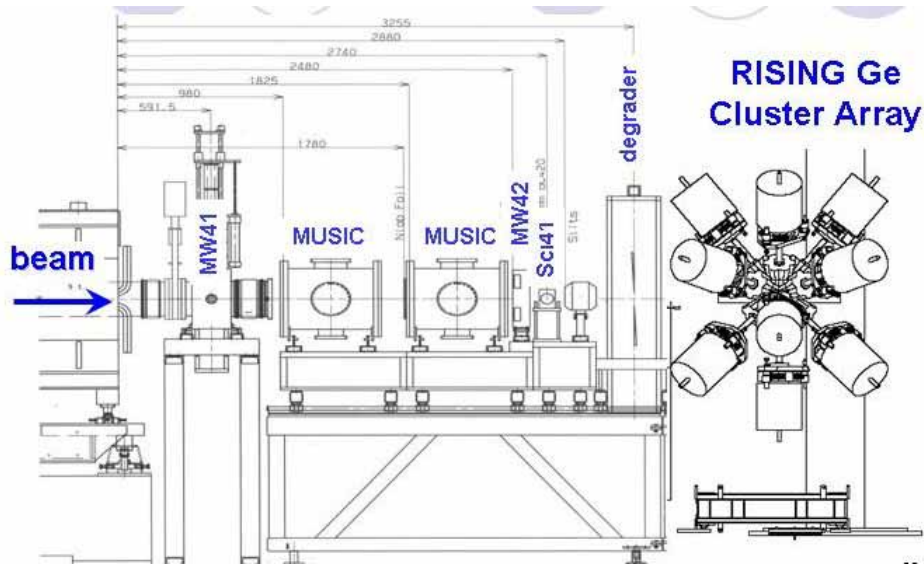


**Fig.17:** Schematic layout of the RISING set-up at the S4 area of the Fragment Separator (FRS) at GSI. The beam diagnostic elements consist of two multiwire detectors (MW41 and MW42), two ionisation chambers (MUSIC) and two scintillation detectors (Sc21 and Sc41). The degrader allows an accurate implantation of the heavy ions in the active stopper, which is surrounded by Ge-cluster detectors for  $\gamma$ -ray measurement.

Two measurements were carried out with the linear and logarithmic MPR-32 preamplifiers. They were placed 30cm away from the DSSSD and combined with two mesytec STM-16 shaping-/timing filter/discriminator modules (at a distance of 10m). The STM-16 units were operated with a gain-value of 1 and a threshold of 20. For the planned decay experiment the optimal settings are a gain-factor of 2 and the threshold as low as possible (e.g. 2-3) to reach the highest efficiency for electron detection. The scintillation detector Sc41 served as a trigger for the measurement.

### 6.1 Results with the linear MPR-32 mesytec preamplifier

The linear MPR-32 preamplifier is well suited for the electron measurement (MeV range), however, for the implantation of heavy ions (GeV range) the output signals saturate. A collection of the measured preamplifier signals can be found in appendix F. The measured energy spectra (10MeV range setting) obtained by x-strips (front junction) of DSSSD-2243-5 are shown in fig.18 for the implantation of  $^{136}\text{Xe}$  ions. They show the low energetic part of the implantation caused by light charged particles and atomic X-rays. In most cases all the strips of the DSSSD fire, since no condition is set on the implantation of the heavy ions. Fig.19 shows the x-strip multiplicity distributions for different energy thresholds. If one takes only the overflow data of the energy spectra ( $>10\text{MeV}$ ), the multiplicity spectrum is localized at small values, which is expected for the implantation. For multiplicity one on each side of DSSSD the position is uniquely determined, while for higher multiplicities the centroid has to be determined. In case of the linear MPR-32 preamplifier each strip has the same weight for this calculation, since the individual strip energies are not measured. Based on the overflow data, a position correlation between the DSSSD and the multiwire detector MW was determined which is displayed in fig.20. The correlation shows that the data measured with the

linearM PR -32 pream plifier can be used for a position determination of the implanted  $^{136}\text{Xe}$  ions.

In conclusion, the overflow data of the DSSSD allow a zero order position determination of the heavy ion implantation.

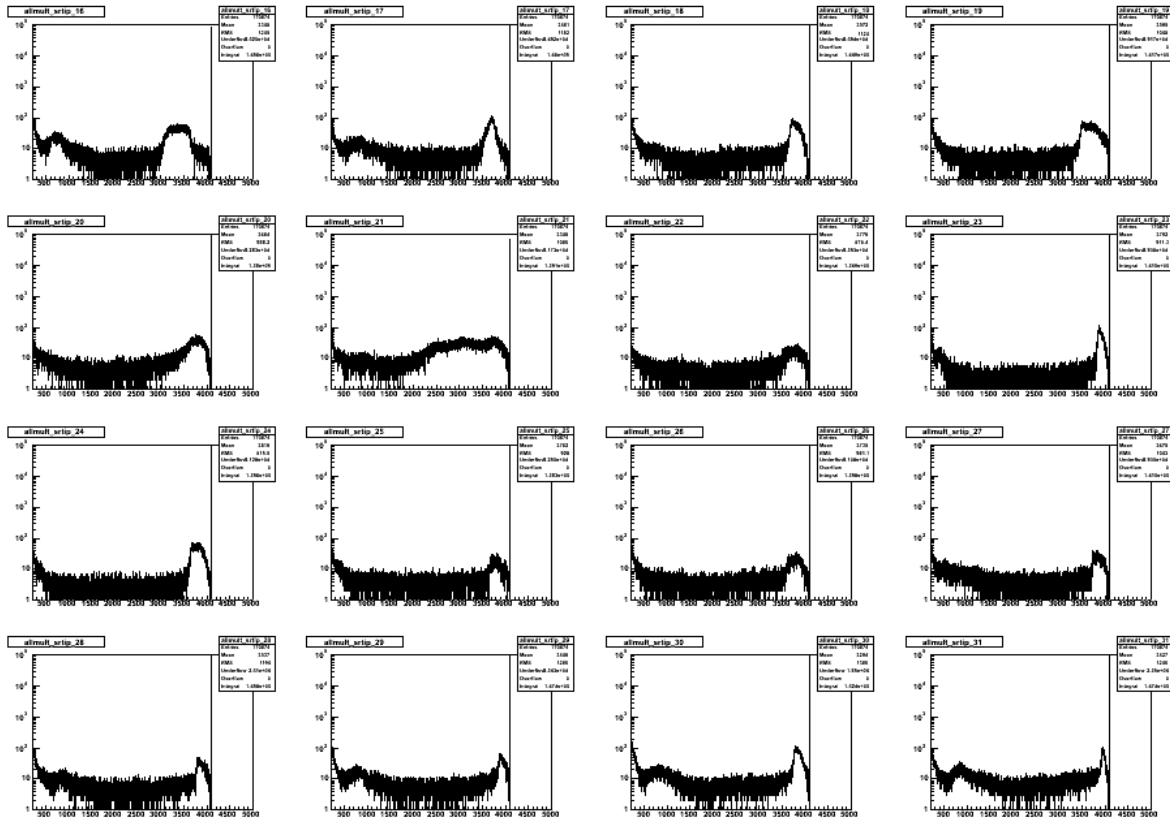


Fig 18: Measured energy spectra (10M eV range of the linearM PR -32 pream plifier) obtained by x-strips (front junction) of DSSSD -2243-5 for the implantation of  $^{136}\text{Xe}$  ions.

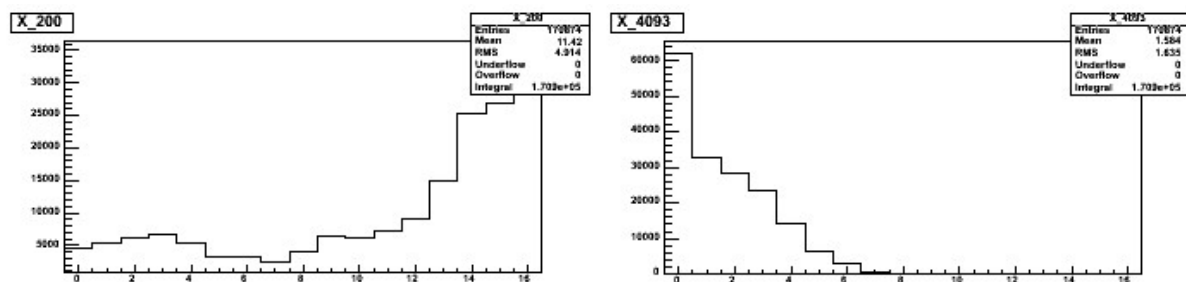
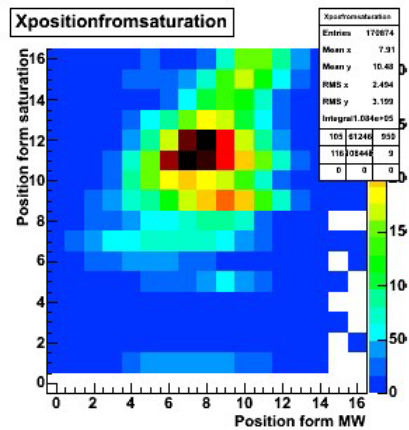


Fig 19: Multiplicity distributions measured by x-strips of DSSSD -2243-5 for different energy thresholds. For a very low threshold (channel number 200) almost all x-strips are firing, while for the overflow (> 10M eV) data the hit probability is very low, as expected for the implantation of  $^{136}\text{Xe}$  ions.



**Fig 20:** Position correlation between the multiwire detector MW and the DSSSD -2243-5. In case of the DSSSD the position of the implanted  $^{136}\text{Xe}$  ion was determined from the overflow data, when a linear MPR-32 preamplifier was used.

## 6.2 Results with the logarithmic MPR-32 mesytec preamplifier

The logarithmic MPR-32 preamplifier is well suited for both the electron measurement (MeV range) and the heavy ion implantation (GeV range). A collection of the measured preamplifier (logarithmic MPR-32) signals and an amplifier (STM-16) signals can be found in appendix G and H, respectively.

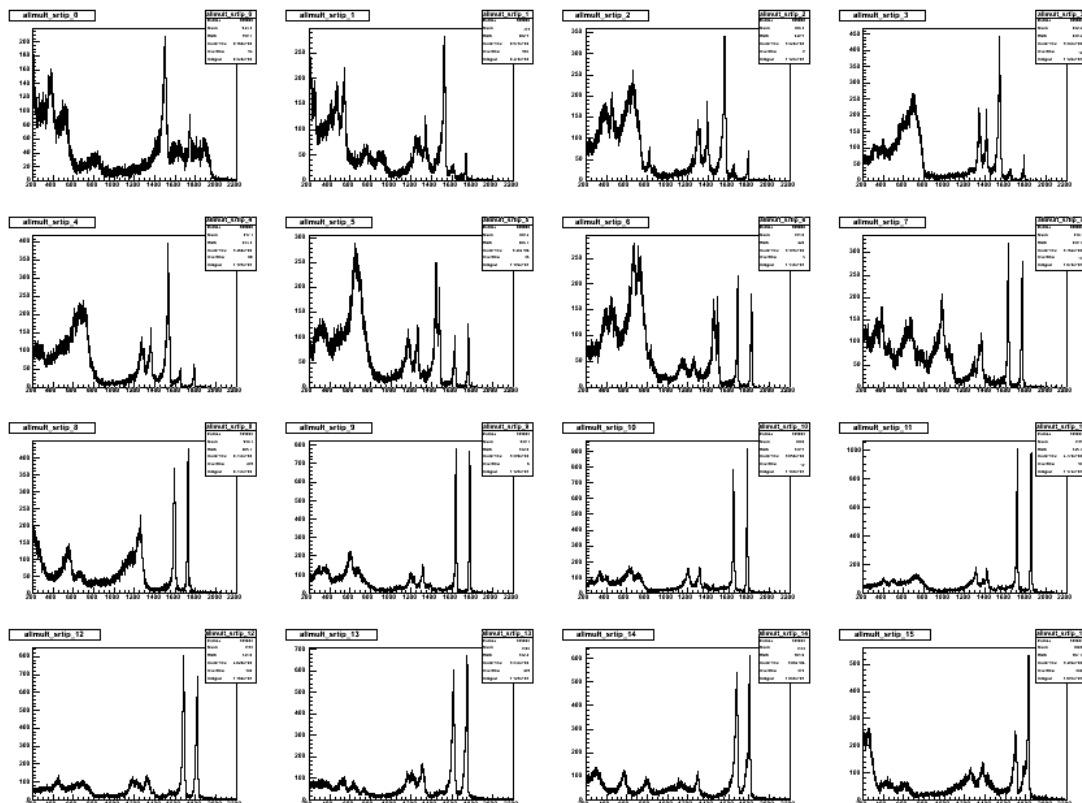


**Fig 21:** Measured energy spectra (10 MeV range for the linear part of the logarithmic MPR-32 preamplifier) obtained by x-strips (front junction) of DSSSD -2243-5 for the implantation of  $^{136}\text{Xe}$  ions. The double hump structure is related to the stopping of the heavy ions.



The measured energy spectra (10M eV range setting for the linear part of the logarithmic preamplifier) obtained by x-strips (front junction) of DSSSD -2243-5 are shown in fig 21 for the implantation of  $^{136}\text{Xe}$  ions. They show a similar distribution at low energy (<10M eV), as compared to the linear MPR-32, and a pronounced double hump structure in the logarithmic part of the spectrum. The double hump structure, which relates to the implantation of the  $^{136}\text{Xe}$  ions, was aligned for each strip and the strip multiplicity for the highest peak was determined. Fig 22 shows the multiplicity distribution for the heavy ion implantation. In most cases only one or two strips on the x- and y-side of DSSSD were activated. It turns out that the highest peak of the double hump structure is related to the implantation, while the second highest peak is interpreted as a cross talk event with the neighbouring strip. The result of the double hump analysis is also displayed in fig 22 showing the hit pattern of the multiplicity 2 events. In 90% of all cases the second highest peak is in a neighbouring strip.

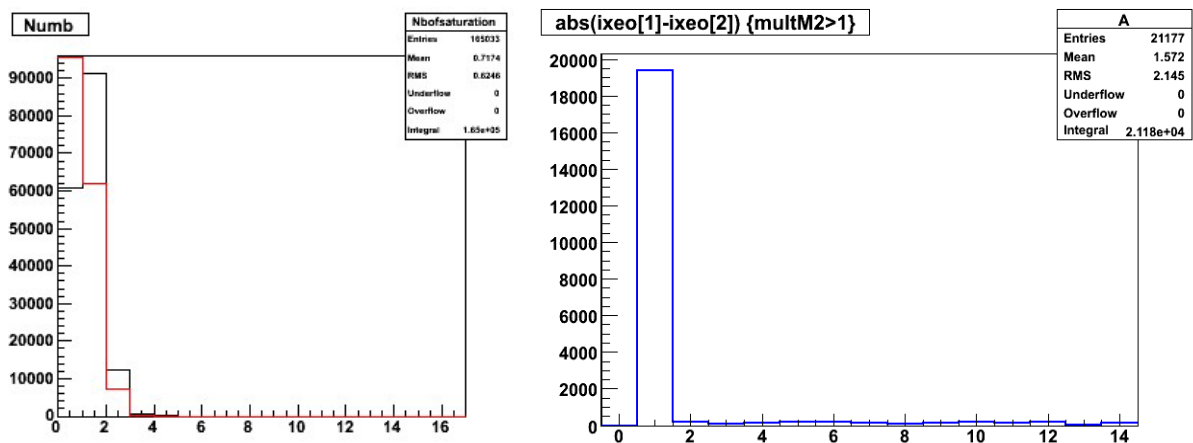


Fig 22: Multiplicity distribution for the higher peak of the double hump structure (left). The black distribution shows the result for all x-strips of DSSSD -2243-5, while for the red one strip=1 was removed, which seemed to be very noisy. The right diagram shows the hit pattern relative to the strip with the highest peak for multiplicity 2 events. In 90% of all cases the second highest peak is in a neighbouring strip.

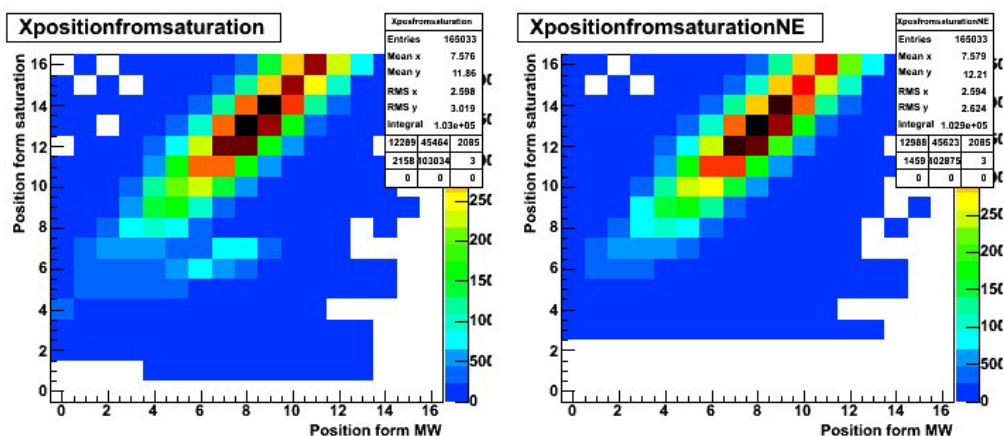


Fig 23: Position correlation between the multiwire detector MW and the DSSSD -2243-5. In case of the DSSSD the position of the implanted  $^{136}\text{Xe}$  ion was determined from the mean of highest peak, when a logarithmic MPR-32 preamplifier was used. The left correlation includes all strips, while for the right one a single noisy strip was removed.

In case of the logarithmic MPR-32 preamplifier the mean of the highest peak of the double hump structure was used for the position determination. In fig 23 the position correlation between the DSSSD and the multiwire detector MW is displayed. It shows a strong correlation but also an offset since the DSSSD was not accurately centred in the frame of the FRS.

In conclusion, the logarithmic MPR-32 preamplifier is recommended to be used for the active stopper measurements.

## References

- [1] Micron Semiconductor Ltd [www.micronsemiconductor.co.uk](http://www.micronsemiconductor.co.uk)
- [2] mesytec [www.mesytec.com](http://www.mesytec.com)
- [3] MultiChannel Systems [www.multichannelsystems.com](http://www.multichannelsystems.com)
- [4] C. Wrede et al., Nucl. Instr. Meth. B204 (2003), 619  
A.C. Schotter et al., Nucl. Instr. Meth. A262 (1987), 353
- [5] J.I. Prisciandaro et al., Nucl. Instr. Meth. A505 (2003), 140
- [6] J. Elson, Pico Systems, 543 Linden Rd., Kirkwood, MO 63122,  
(314)-965-5523 [elson@pico-systems.com](mailto:elson@pico-systems.com) [pico-systems.com/shapdisc.html](http://pico-systems.com/shapdisc.html)

## Appendix A



Rear Ohmic Side  
Front Junction Side







**Micron Semiconductor**

N° Junction Elements:	16
N° Junction Elements:	16
Element Length:	49.5 mm
Element Pitch:	3.1 mm
Element width:	3.0 mm
Active Area:	60x60 mm <sup>2</sup>
Thickness:	1000 µm
Price:	5800 €



**MPR-32**  
Charge Sensitive Preamplifier

32 channel compact module	
Sensitivity switch, factor 5	
Bias voltage up to ±400V	
Price:	2790 €



**STM-16**  
16 fold shaper

16 channel NIM module	
shaper amplifier	
timing filter amplifier	
leading edge discriminator	
Price:	2x3415 €



**ADC V785AF**  
32 channel

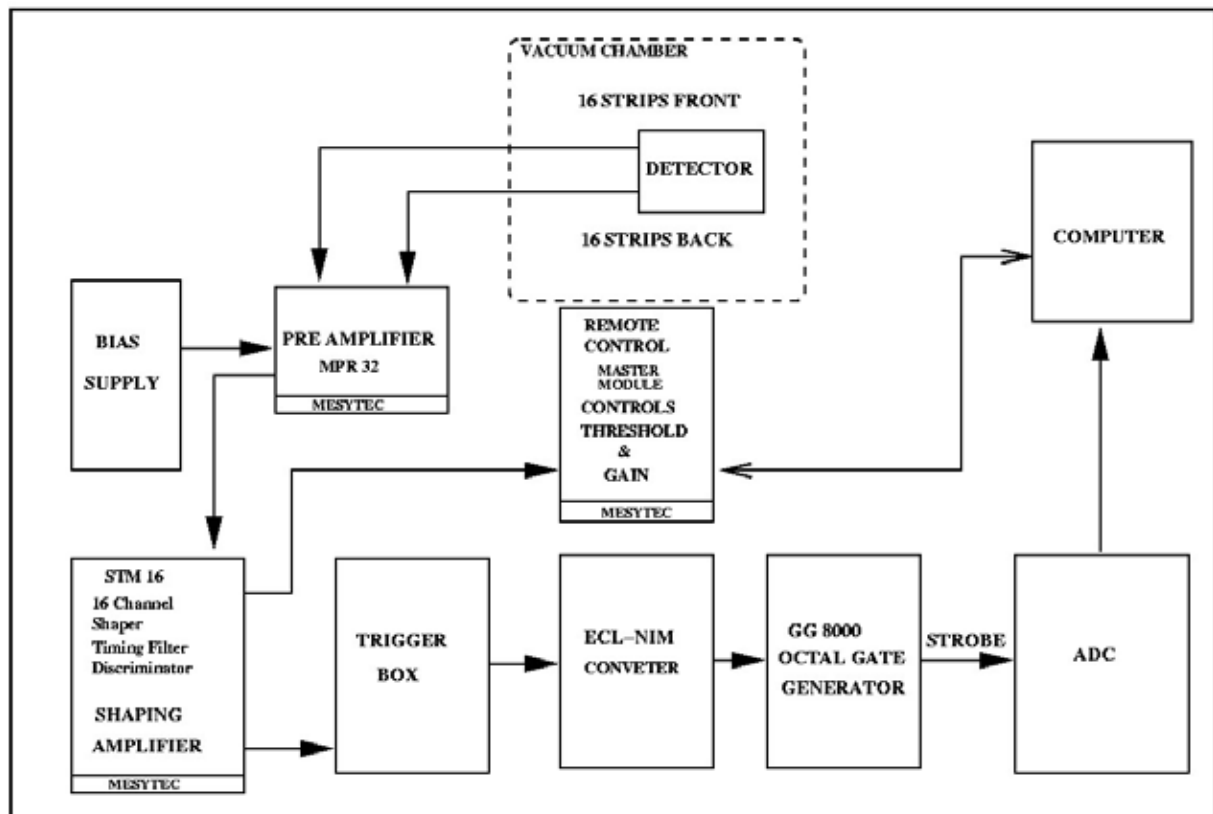
Price:	5094 €
--------	--------

**Total cost 22,514.- €**

<b>MRC-1</b> remote master controller for STM-16	
Price:	2200 €



## Appendix B : Block diagram using mesytec electronics



## Appendix C

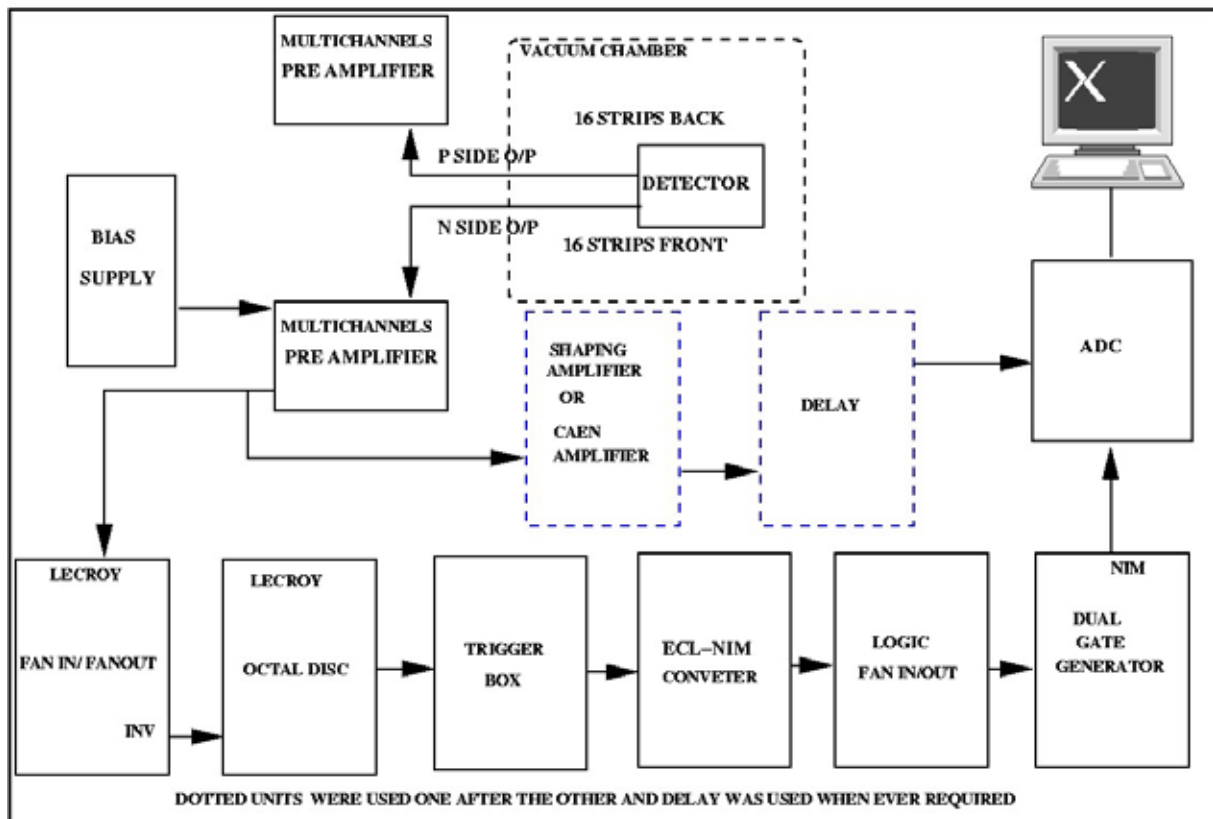
**Micron Semiconductor**

N° Junction Elements: 16	CPA-16	Amplifier N 568BC	ADC V785AF
N° Junction Elements: 16	Charge Sensitive Pre amplifier	16 fold shaper	32 channel
Element Length: 49.5 mm	16 channel compact module	Price: 2x3481 €	Price: 2x 5094 €
Element Pitch: 3.1 mm	2 output stages with different gains		
Element width: 3.0 mm	Bias voltage up to $\pm 500V$		
Active Area: $50 \times 50 \text{ mm}^2$	Price: 2x2250 €		
Thickness: 1000 $\mu\text{m}$			
Price: 5600 €			

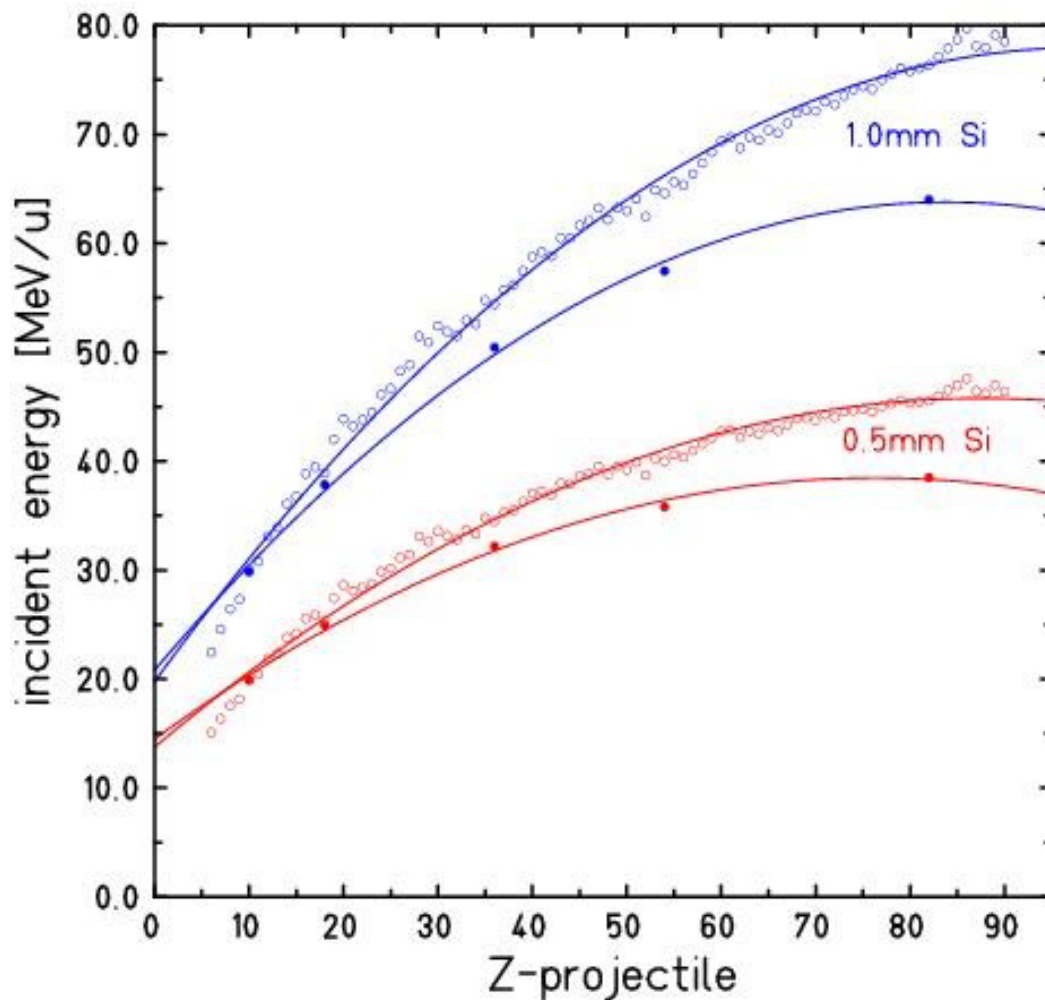
**Total cost 27,250.- € (discriminator not included)**



## Appendix D : Block diagram using MultiChannelSystem s electronics



Appendix E : Maximum incident energy for heavy ions implanted in 0.5 mm and 1 mm silicon



Projectiles are implanted in 0.5 mm (116.5 mg/cm<sup>2</sup>) and 1 mm (233 mg/cm<sup>2</sup>) silicon. The maximum incident energy [MeV/u] is determined from the range tables of F. Hubert et al. *Annales de Physiques* 5 (1980), p.1 (open symbols) and from ranges calculated using the ATIMA code (full symbol).

F. Hubert et al.

$$1.0 \text{ mm Si: } E = 19.772 + 1.18791 * Z - 0.00606377 * Z^2$$

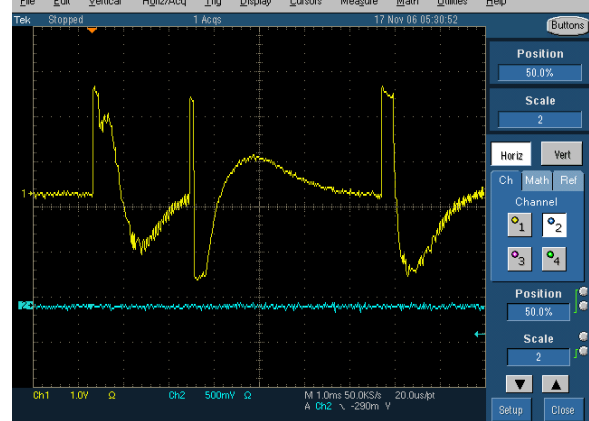
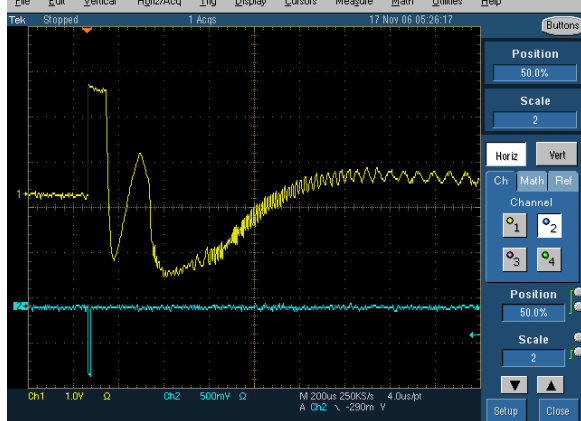
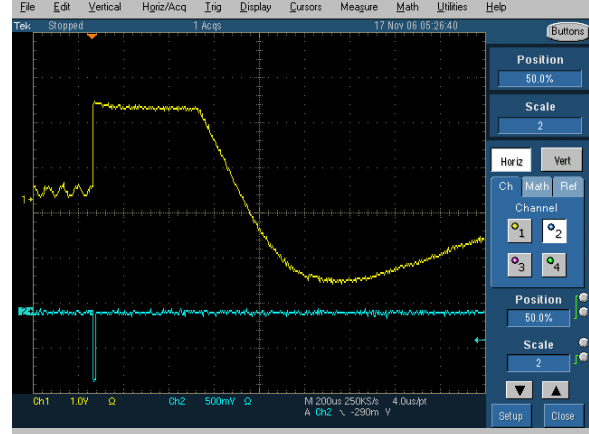
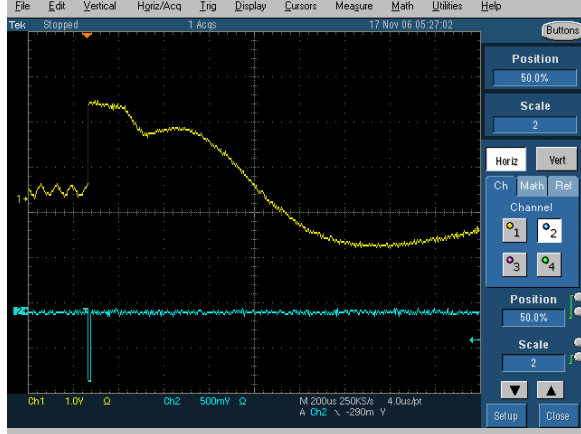
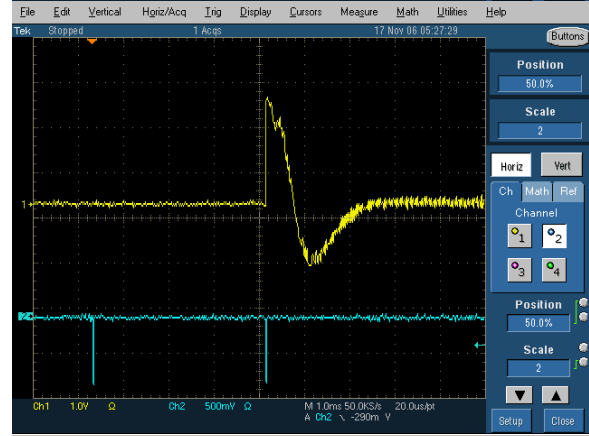
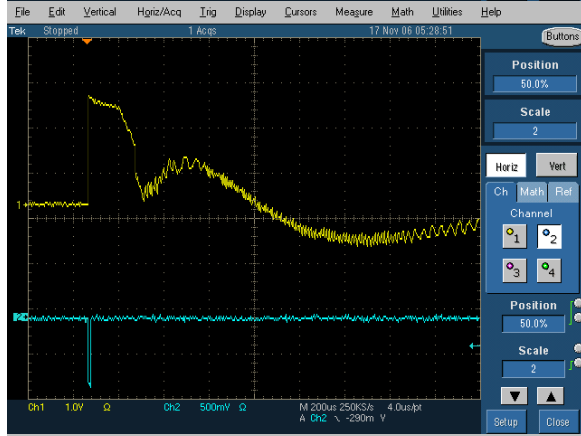
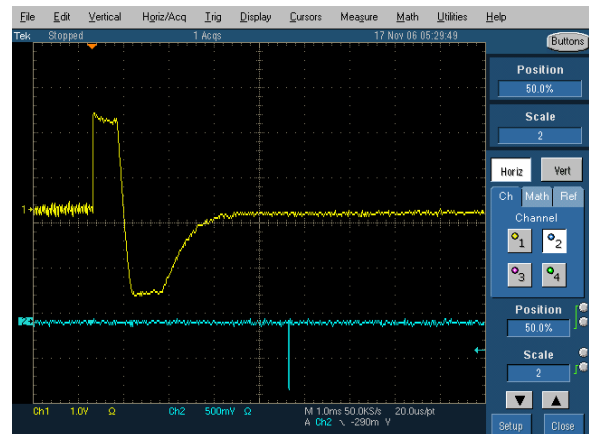
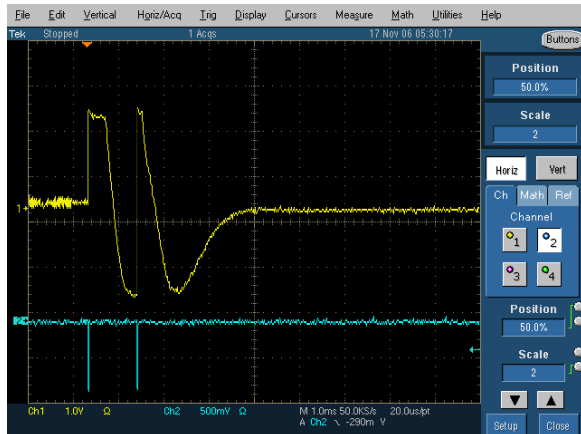
$$0.5 \text{ mm Si: } E = 13.738 + 0.73188 * Z - 0.00417978 * Z^2$$

ATIMA

$$1.0 \text{ mm Si: } E = 20.803 + 1.02507 * Z - 0.00611181 * Z^2$$

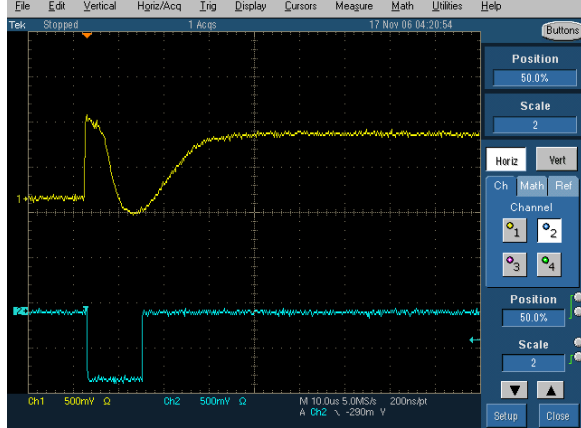
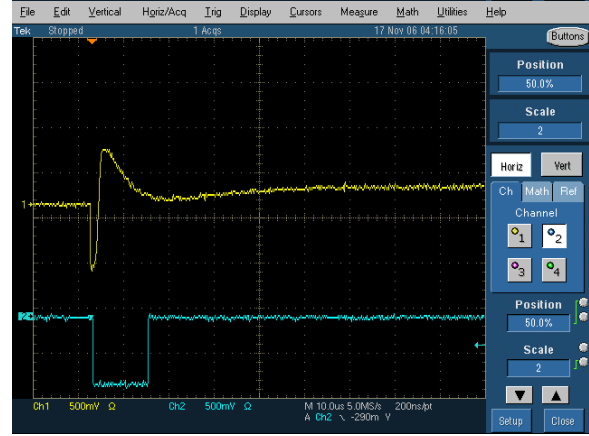
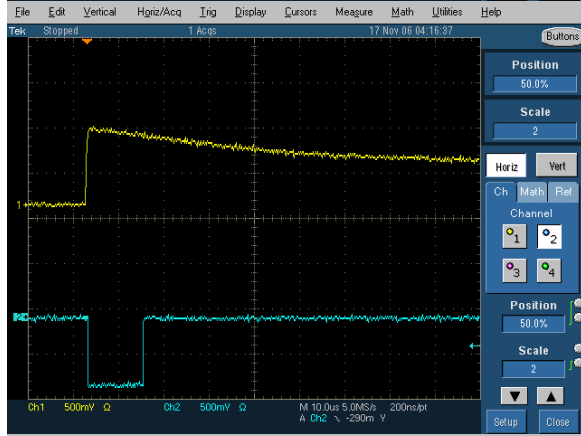
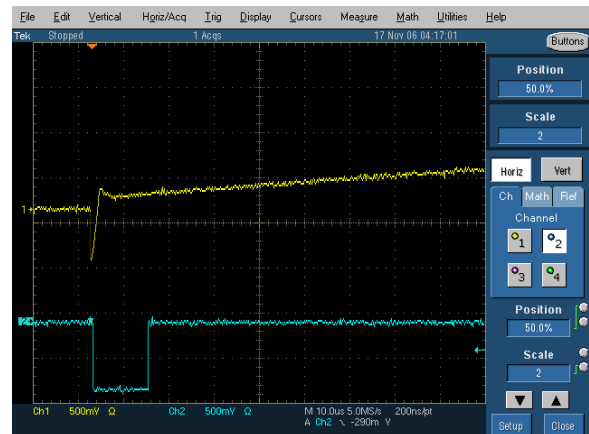
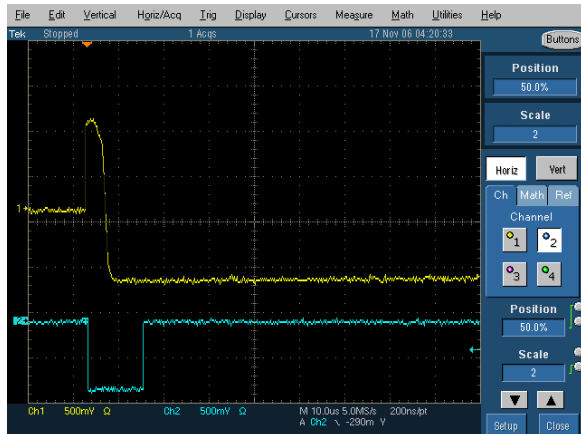
$$0.5 \text{ mm Si: } E = 14.487 + 0.62831 * Z - 0.00411604 * Z^2$$

# Appendix F : Pre-amplifier signals measured with MPR-32 (lin)

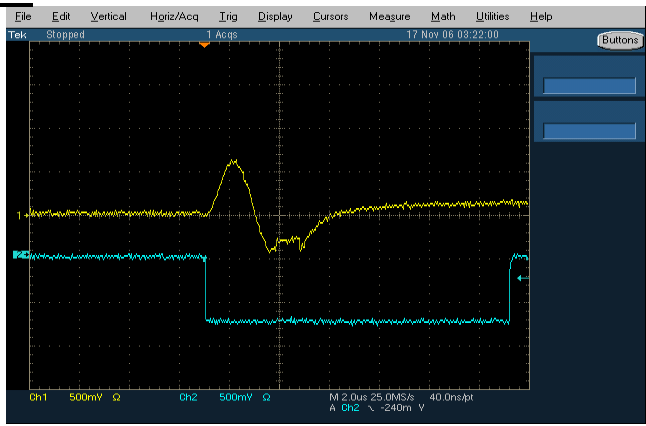
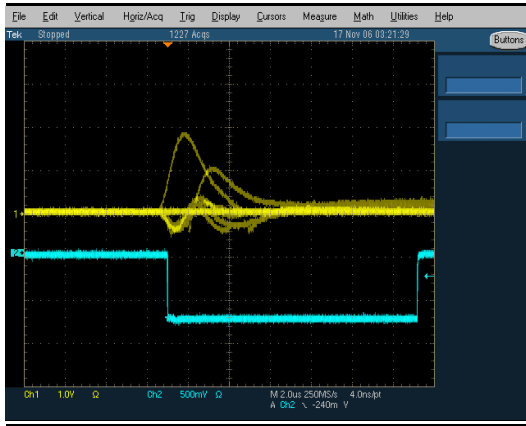
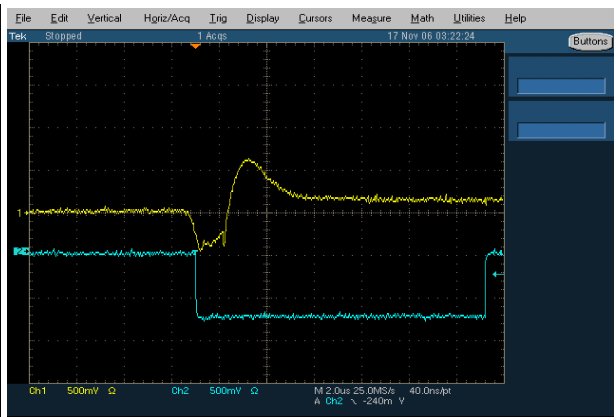
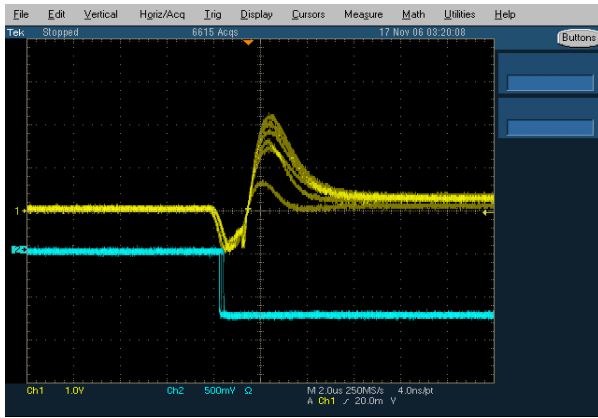




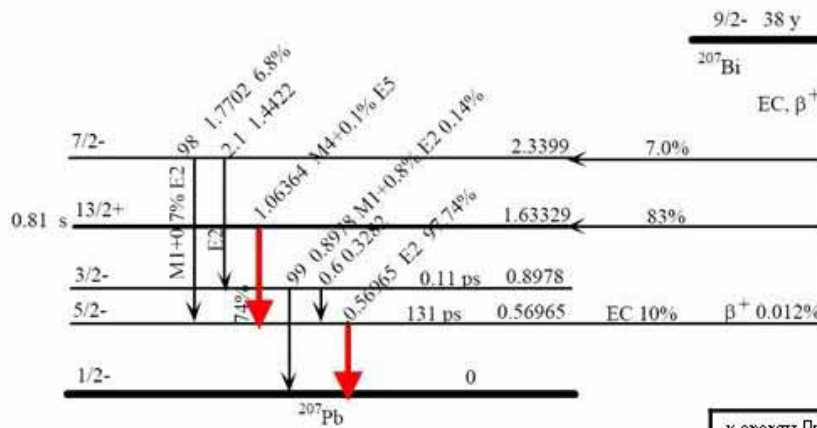
# Appendix G : Pre-am plifier signalsm easured w ith M PR -32 (log)



# Appendix H : Amplifier signals measured together with MPR-32 (log)



# Appendix I: Decay scheme of $^{207}\text{Bi}$



$\gamma$ -energy [keV]	e <sup>-</sup> -energy
569.6	481.7 [K]
	553.8-556.7 [L]
	565.8-567.2 [M]
1063.7	975.7 [K]
	1047.8-1050.6 [L]
	1059.8-1061.2 [M]

$^{207}\text{Bi}$  emits gamma rays and electrons